

First direct detection of an RR Lyrae star conclusively associated with an intermediate-age cluster

Cecilia Mateu¹ , Bolivia Cuevas-Otahola², and Juan José Downes¹

¹ Departamento de Astronomía, Instituto de Física, Universidad de la República, Iguá 4225, CP 11400 Montevideo, Uruguay

² Departamento de Matemáticas, FCE, Benemérita Universidad Autónoma de Puebla, Puebla, 72000, México

Received September 15, 1996; accepted March 16, 1997

ABSTRACT

Context. RR Lyrae stars have long been considered unequivocal tracers of old (>10 Gyr) and metal-poor ($[\text{Fe}/\text{H}] < -0.5$) stellar populations. First, because these populations are where they are readily found and, according to canonical stellar evolution models for isolated stars, these are the only populations where RR Lyrae should exist. Recent independent results, however, are challenging this view and pointing at the existence of intermediate-age RR Lyrae, only a few (2–5) Gyrs old.

Aims. Our goal in this work is to provide direct evidence of the existence of intermediate-age RR Lyrae by searching for these stars in Milky Way open clusters, where the age association will be direct and robust.

Methods. We searched over 3,000 open clusters with published kinematically associated member stars from Hunt & Reffert (2024) by crossmatching against a compilation of the largest publicly available RR Lyrae surveys (*Gaia*, ASAS-SN, PanStarrs1, Zwicky Transient Factory and OGLE-IV).

Results. We identified a star as a bona fide RR Lyrae variable and robust member of the 2–4 Gyr old Trumpler 5 cluster, based on its parallax and proper motions and their agreement with confirmed cluster members. We derived an extremely low probability ($0.049 \pm 0.013\%$) that the star is a background field RR Lyrae and provide initial constraints on a possible binary companion based on its position in the colour-absolute magnitude diagram.

Conclusions. Currently a source of debate, the Trumpler 5 RR Lyrae provides the most direct evidence to date of the existence of RR Lyrae stars at much younger ages than traditionally expected and adds to the mounting evidence supporting their existence.

Key words. XX – XX – XX

1. Introduction

RR Lyrae (RRL) stars are classical pulsator core He-burning stars produced at the intersection of the instability strip and the horizontal branch. A convenient combination of observational properties have made them an extremely popular tracer of Milky Way (MW) structure in the current era of deep, large-scale, synoptic photometric surveys. Due to their distinctive variability they are easily and reliably identified based on (multi-epoch) photometry alone; and their standard candle nature provides individual distances with excellent precisions (down to a few percent), which, coupled with their large luminosities have made them ideal tracers of the tridimensional structure of our Galaxy and its surroundings (see e.g. Zhang et al. 2025; Prudil et al. 2025; Cabrera-Gadea et al. 2025; Ngeow & Bhardwaj 2025; Medina et al. 2024; D’Orazi et al. 2024).

Recent studies are defying the canonical notion that RRLs are tracers of exclusively old and metal-poor populations (e.g. Catelan & Smith 2015; Smith 1995). In the first large scale study of RRL kinematics in the MW using *Gaia* DR2 (Gaia Collaboration et al. 2018), Iorio & Belokurov (2021) found a significant population of metal-rich RRLs ($[\text{Fe}/\text{H}] \gtrsim -0.5$ up to nearly solar) with kinematics resembling thin disc populations 2–5 Gyrs old, much colder and faster-rotating than observed for disc populations at > 10 Gyrs, the age expected for canonical RRL. Nearly simultaneously, in an independent study, Sarbadhicary

et al. (2021) concluded that almost half (51%) the RRLs in the Large Magellanic Cloud (LMC) are associated to intermediate-age populations with ages from 1.2 to 8 Gyrs. Their study was based on the Delay Time Distribution (DTD) of RRLs, a measure of the number of objects per unit (initial) mass formed after a burst of star formation, inferred from the spatial distribution of RRLs and a map of the stellar age distribution across the LMC. Both studies, based on completely independent data and methods, pointed at the existence of intermediate-age populations of RRLs only a few Gyrs old, much younger –and in the case of the MW, also more metal-rich– than could be explained by canonical stellar evolution models. More recent studies of the kinematics of RRLs in the Galactic disc’s warp (Cabrera-Gadea et al. 2025) and of the correlation of the kinematics of RRL and Mira stars of different ages determined via the Mira’s period-age relation (Zhang et al. 2025) have further supported the kinematical intermediate age of thin disc RRLs found by Iorio & Belokurov (2021).

Although these studies strongly support the existence of intermediate-age RRL stars, their conclusions rely on indirect age estimates and/or statistical inferences about the expected fraction of such stars. This highlights the need for a direct and unambiguous identification of individual RRLs associated with an intermediate-age cluster, where the age association is unequivocal. Such objects will provide key constraints to the evolutionary channels that are being proposed to explain the existence of these objects, e.g. by stellar population synthesis models in

* cmateu@fcien.edu.uy

cluding binary evolution with mass transfer (Karczmarek et al. 2017; Bobrick et al. 2024).

In Cuevas-Otahola et al. (2025) we conducted a search for RRLs associated to intermediate-age clusters in the Magellanic Clouds (MCs), in an attempt to find direct evidence confirming the existence of these stars at such early ages. The search yielded 23 RRL possible members in 10 clusters with ages from 2 to 8 Gyrs. Given how distant the clusters are, the current precision of *Gaia* DR3 proper motions is not yet enough to offer conclusive kinematic memberships and about half the RRL are expected to be field contaminants from the MC’s population, awaiting spectroscopic follow-up for radial velocities to confirm their memberships to the clusters.

In the MW the vast majority of clusters found at ages younger than 8 Gyrs are open clusters (OCs) whose masses are typically $< 10^3 M_\odot$ (with a handful of Young Massive Clusters having larger masses, Portegies Zwart et al. 2010). The present-day formation rate (PTF) of $0.83 \text{ RRLs}/10^5 M_\odot$ found by Cuevas-Otahola et al. (2025) for clusters in that age range implies only 1 in a few thousand clusters is statistically expected to host a single RRL and that a search over a large sample of several thousand clusters is warranted. Such a search has become feasible thanks to *Gaia*, which has enabled millions of stars to be catalogued as members of a vast number of OCs (over 5,000) with kinematic membership probabilities robustly estimated based on parallax and proper motions (e.g. Hunt & Reffert 2023; Cantat-Gaudin et al. 2018, 2020). A quick estimate from the cluster masses reported by Hunt & Reffert (2024) and the Cuevas-Otahola et al. (2025) inferred rates yields a total mass of $\sim 4 \times 10^5 M_\odot$ for the 172 clusters in the age range from 1 to 8 Gyrs, which implies $\sim 2\text{--}3$ RRLs could be lurking in the population of known Galactic OCs.

In this work we present *the first RRL star conclusively associated to an intermediate age population: the 2–4 Gyr-old cluster Trumpler 5*. In Sec. 2 we describe our search, conducted with a compilation of public RRL surveys crossmatched against the catalogue of stellar members associated to OCs from Hunt & Reffert (2023). Our search resulted in an initial sample of 15 candidates, out of which we confirm one star as a bona fide RRL. In Sec. 3 we show the star to be robustly identified as an RRL, and as a cluster member by comparing it against cluster member’s parallax, kinematics and position in the colour-magnitude diagram (CMD), and by showing that it has an extremely low probability ($0.049 \pm 0.013\%$) of being a background field RRL. In Sec. 4 we discuss constraints on a possible binary companion based on its position in the CMD and the spectral energy distribution (SED), and Trumper-5 as a cluster which favours stellar evolution with mass transfer. We present our conclusions in Sec. 5.

2. Data

In this work we use the OC census from Hunt & Reffert (2023) with mean cluster parameters from their Table 3 and members data from Appendix A of Hunt & Reffert (2024). In this latter work, the census from Hunt & Reffert (2023) was updated by including colour-magnitude diagram information in the cluster classification scheme and reporting extinction, age and distance based on isochrone fitting, as well as Jacobi radius and stellar mass for each cluster.

For the RRLs we use the catalogue described in Cabrera-Gadea et al. (2025) which combines the *Gaia* DR3 SOS catalogue from Clementini et al. (2023), the PanSTARRS1 (PS1) catalogue from Sesar et al. (2017a) and the ASAS-SN from Jayas-

inghe et al. (2019a,b), augmented with crossmatches against the Zwicky Transient Facility (ZTF) and the Optical Gravitational Lensing Experiment (OGLE) IV catalogues from Chen et al. (2020) and Soszyński et al. (2016), respectively, following the crossmatching strategy described in Cabrera-Gadea et al. (2025). The final *GAPZO* catalogue contains a total of 309,998 RRL stars spanning the full sky.

For our analysis we crossmatched the *GAPZO* RRL catalogue by *Gaia* DR3 `source_id` against the OC member table from Hunt & Reffert (2024), keeping the 3,530 clusters classified strictly as OCs (`Type='o'`) to avoid globular clusters and moving groups, and with `CMDC150>= 0.5` and `CST> 5` in order to keep only reliable OCs as suggested by Hunt & Reffert (2023), and limiting our search to members within each cluster’s tidal radius. This results in a sample of 3,358 young (< 1 Gyr) and 172 intermediate age clusters (1–8 Gyr), in which an initial number of 15 RRLs were identified as members of the same number of OCs. Out of these, 13 stars were identified as RRL by a single survey, one by two surveys (ZTF and *Gaia*) and the last one by all five surveys. Based on visual inspection of their light curves and position in the CMD, 14 out of the 15 stars were discarded based on their light curves (the majority were reclassified as eclipsing binaries) and/or their position in the CMD, as described in detail in Appendix A. In what follows, our discussion will focus on the last standing RRL star.

3. Results: The RRL star in Trumpler 5

Our search resulted in one star robustly identified as an RRL and as a member of an intermediate-age OC, the Trumpler 5 cluster. The RRL is identified as `source_id=3326852328563919744` by *Gaia* DR3. *Gaia* DR3 astrometric parameters (Gaia Collaboration et al. 2023) for the RRL and physical and astrometric parameters for the cluster from several sources are summarised in Table 1.

Anderson & Hunt (2025) recently conducted a similar search for variable stars in the Hunt & Reffert (2023) OC census by crossmatching against the *Gaia* DR3 Specific Objects Study (SOS) catalogues for different classes of variable stars and found two stars classified as RRLs by *Gaia*. Upon inspection of their light curves and position on the CMD, the stars turned out to be likely eclipsing contact binaries and, consequently, the authors concluded no RRLs were found associated to OCs. Their search, however, was motivated by their study of much less luminous classes of variables and their sample limited to clusters nearer than 2.5 kpc, a limitation we did not need to impose here.

3.1. A bona fide RRL

The star is consistently reported as an RRab in all five surveys in the *GAPZO* catalogue. Table 2 summarises its main light curve parameters and Figure 1 shows the star’s light curves (top row) in the 9 different filters for the 4 surveys with publicly available time series data. In all cases the light curves show the typical sawtooth shape expected from its classification as an RRL of type ab. As observed in Figure 1 and Table 2, amplitudes decrease as filters become redder, as expected for a pulsating star (e.g. Kinman & Brown 2010; Catelan & Smith 2015), except for the V-band amplitude from ASAS-SN. The location of the star in the Period-Amplitude diagram (bottom row) for all bands is consistent with the expectation from the Period-Amplitude anti-correlation in all 8 bands available for *Gaia*, PS1 and OGLE-IV (only one band per survey is shown). For ASAS-SN the relatively low V-band amplitude places the star below the main

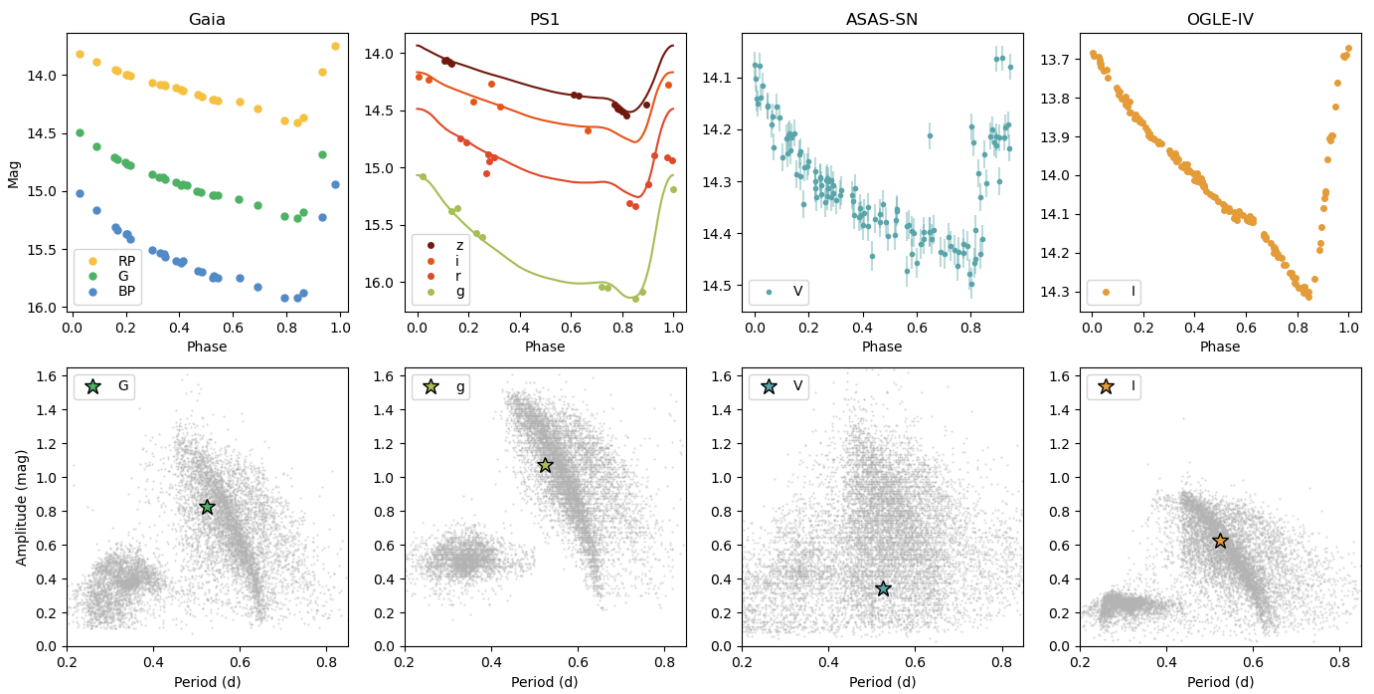


Fig. 1. Phase-folded light curves (top row) and location of the Trumpler 5 RRL in the Period-Amplitude diagram (bottom row) for the four surveys with publicly available time series data, from left to right: *Gaia* (Clementini et al. 2023), *PS1* (Sesar et al. 2017b), *ASAS-SN* (Jayasinghe et al. 2019a) and *OGLE-IV* (Soszyński et al. 2016). In the bottom row the location of the Trumpler 5 RRL (star symbol) is shown in comparison to RRLs from each survey in the selected band. See text for details. Error bars for the magnitudes are plotted in all panels in the top row but are smaller than the symbol size in all cases except for *ASAS-SN*.

locus, however, the overall distribution for *ASAS-SN* RRL is much more scattered than usually observed, which is also reflected in a much weaker Period-Amplitude anti-correlation, in turn leading to lower amplitudes being more common in this catalogue (Catelan & Smith 2015). This suggests the low amplitude is more likely due to *ASAS-SN* amplitudes having a tendency to be underestimated, rather than it having a more physical explanation like the RRL being a Blahzko star, which may have explained its lower amplitude. We therefore conclude the star's observed light curve, period and amplitudes are typical for an RRab.

3.2. Kinematic Cluster Membership

Figure 2 shows the RRL star's position relative to cluster members from Hunt & Reffert (2024), from left to right, in the sky and proper motion planes, in a parallax histogram and in the color-magnitude diagram (CMD), using *Gaia* bands. As shown by the figure, the RRL lies within the cluster's tidal radius (by construction of our search) and its proper motions and parallax are in excellent agreement with the cluster's, supporting its likely membership at face value.

Our Trumpler 5 RRL was identified by Hunt & Reffert (2023) as a member of the cluster with a membership probability $p = 0.51$. The star had also been previously identified as a member of Trumpler 5 by Cantat-Gaudin et al. (2018, 2020) using *Gaia* DR2 and van Groeningen et al. (2023) using *Gaia* DR3, with probability 1 in all cases. All of these works compute membership probabilities by modelling the cluster in the same space of observables (sky, parallax and proper motions) with a key difference being that membership probabilities from Hunt & Reffert (2023) were computed using HDBSCAN. According to the authors their algorithm does not take into account observational

errors and bases the assignment of probabilities on the proximity of a given star to the bulk of the cluster's population, in contrast to the works of Cantat-Gaudin et al. (2018, 2020) and van Groeningen et al. (2023) in which observational uncertainties are accounted for, which may explain the much lower membership probability found for this star by Hunt & Reffert (2023). Since this point is key, in Sec. 3.4 we revisit it and show the probability that the star may be a chance interloper of the thin disc field population is extremely low.

Finally, an exhaustive search of major spectroscopic survey databases (DESI, LAMOST, SDSS-IV) as well as using Simbad and VizieR yielded no available measurements for the star's line-of-sight velocity in the literature.

3.3. Metallicity and location in the CMD

The star's photometric metallicity, estimated from the Fourier light curve ϕ_{31} parameter, has been reported by Clementini et al. (2023) as $[\text{Fe}/\text{H}] = -0.44 \pm 0.34$, by Li et al. (2023) as -0.86 ± 0.33 , by Muraveva et al. (2025) based on the *Gaia* DR3 G-band, and as -0.98 ± 0.45 and -0.71 ± 0.22 by He et al. (2025) from ZTF *g* and *i* bands. The dispersion between the measurements, particularly of those inferred from the same data, shows that photometric metallicity estimates are still quite imprecise in an individual basis. In the last three cases, although slightly more metal-poor than the cluster's, all estimates are deviated by $\leq 1.4\sigma$ from the cluster's spectroscopic metallicity of $[\text{Fe}/\text{H}] = -0.4$ (Donati et al. 2015). We therefore take the RRL's metallicity as being consistent with the cluster's within its uncertainties.

The RRL's position in the CMD is also shown in Figure 2 (last panel), where a remarkable agreement is found between the star's apparent *G*-band magnitude and that *expected* for the HB

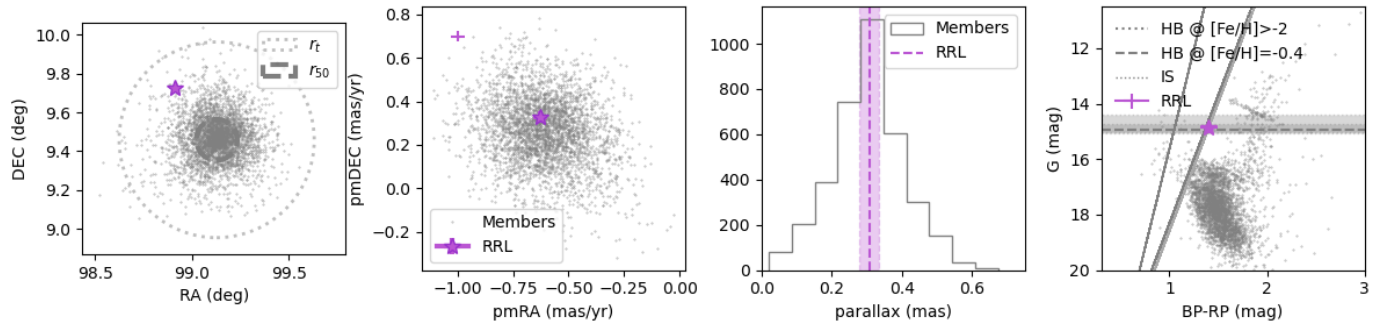


Fig. 2. The Trumpler 5 RRL (star) and cluster members (light gray) are shown, from left to right, in the plane of the sky (DEC versus RA), proper motions (pmDEC versus pmRA), parallax and *Gaia* CMD. In the first panel, r_t and r_{50} are shown with the dotted and dashed lines, these correspond respectively to the tidal radius and radius enclosing 50% of the members according to Hunt & Reffert (2023). In the fourth panel, the solid lines correspond to instability strip (IS) limits from Cruz Reyes et al. (2024) with He abundances from $Y = 0.22$ to $Y = 0.395$; the dotted line shows the *expected* apparent G-band magnitude of the HB at the cluster's metallicity ($[Fe/H] = -0.4$, Donati et al. 2015), and its distance and extinction according to Hunt & Reffert (2024); the shading represents the uncertainty in the HB luminosity corresponding to $\Delta[Fe/H] = 0.5$ dex. The agreement with the RRL's apparent magnitude is remarkable and the star lies right at the edge of the (empirical) limits of the IS (Cruz Reyes et al. 2024).

Table 1. Astrometric and physical parameters for the Trumpler 5 cluster and the RRL star

Trumpler 5 Cluster	
(RA,DEC)	(99.12705764, +9.45854713) deg
(l, b)	(202.82, +1.02) deg
Parallax	(0.302 ± 0.002) mas
pmRA*	(-0.618 ± 0.003) mas/yr
pmDEC	(0.269 ± 0.002) mas/yr
Mass	(2.46 ± 0.17) $\times 10^4 M_\odot$
Age	2.2 – 4.2 Gyr 2.5 Gyr (O25) ($2.17^{+1.00}_{-0.70}$) Gyr (H23) (3.5 ± 1.7) Gyr (D21) 4.2 Gyr (CG20)
Distance	($2.905^{+0.010}_{-0.009}$) 3.047 kpc (CG20)
[Fe/H]	-0.403 ± 0.006 (D15)
A_V	(1.71 ± 0.19) mag (H23)
r_t	(0.50 deg, 25.5 pc)
r_c	(0.077 deg, 3.9 pc)
r_{50}	(0.11 deg, 5.4 pc)
RRL	
source_id	3326852328563919744
(RA,DEC)	(98.90796904, 9.72592814) deg
(l, b)	(202°48, 0°95) deg
Parallax	(0.306 ± 0.028) mas
pmRA*	(-0.627 ± 0.031) mas/yr
pmDEC	(0.328 ± 0.026) mas/yr
G	(14.874 ± 0.012) mag
ruwe	1.1
BEP	1.3

Notes. Reference legend: O25=Özdemir et al. (2025), H23=Hunt & Reffert (2023), D21=Dias et al. (2021), CG20=Cantat-Gaudin et al. (2020), D15=Donati et al. (2015).

assuming the cluster's metallicity of $[Fe/H] = -0.403 \pm 0.006$ (Donati et al. 2015), its distance and extinction $A_V = 1.64$ from Green et al. (2019) and assuming the absolute magnitude versus metallicity relation for the G band from Garofalo et al. (2022, Eq. 13). The empirical limits of the IS accord-

Table 2. Period, light curve amplitudes and (intensity averaged) mean magnitudes for the Trumpler 5 RRL

Survey	Period (d)	Band	Amplitude (mag)	MeanMag (mag)
<i>Gaia</i> SOS	0.524806	<i>BP</i>	1.07	15.50
		<i>G</i>	0.82	14.87
		<i>RP</i>	0.69	14.09
ASAS-SN	0.524830	<i>V</i>	0.34	14.31
PS1	0.524815	<i>g</i>	1.07	15.84
		<i>r</i>	0.77	15.00
		<i>i</i>	0.61	14.53
		<i>z</i>	0.58	14.28
ZTF	0.524790	<i>r</i>	0.81	14.88
OGLE	0.524807	<i>I</i>	0.62	13.99

Notes. References are those provided for each survey in Sec. 2.

ing to Cruz Reyes et al. (2024) for normal and extreme values of globular cluster's He abundances are also shown. Finally, we searched *Gaia* DR3 flags `ipd_frac_multi_peak` and `ipd_gof_harmonic_amplitude` for signs of potentially unresolved binarity (Lindegren 2018) but found none. Also the star's `RUWE` and `phot_bp_rp_excess_factor` are normal as shown in Table 1.

3.4. Not a background RRL star

Our argument that this a bona fide intermediate-age RRL star hinges on a reliable association to the cluster. A definitive association would require a measurement of the star's radial velocity, currently unavailable. In the mean time, we can assess how likely it is that our star is a chance interloper from the field population.

We quantify the probability that a field MW RRL has proper motions and parallax compatible with our star's. For reference, within the cluster's projected tidal radius of ~ 0.5 there are only three other RRLs. Hence, a large window is necessary to include enough RRLs for the background to be modelled properly, which already hints the likelihood of chance interlopers is very low. We select a window such that at least 2000 RRL are included, which resulted in a radius of $\sim 25^\circ$. Figure 3 shows the distribution of all field stars, field RRLs, cluster members and the RRL

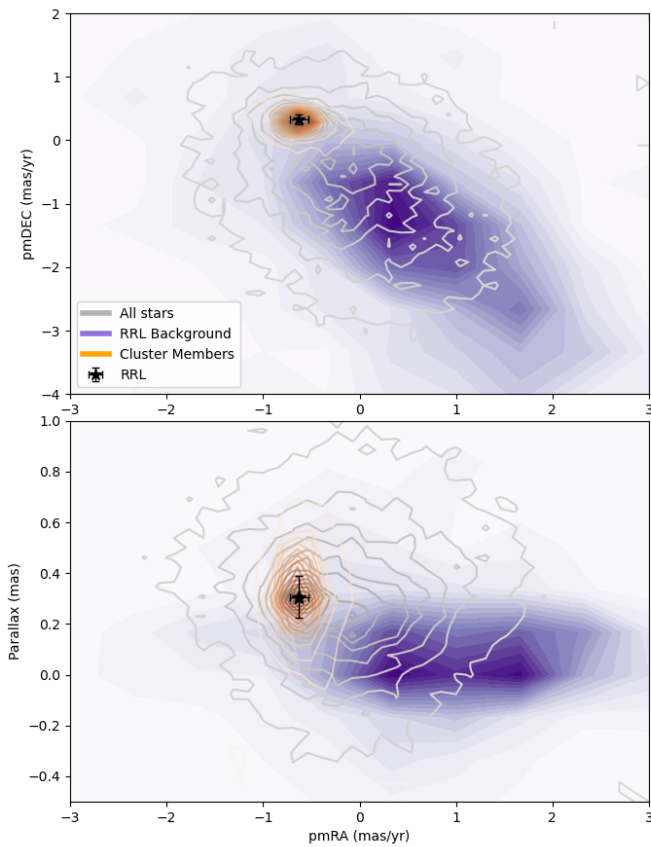


Fig. 3. Location of the Trumpler 5 RRL (black star) with respect to the field population in the proper motions (top panel) and parallax versus pmRA (bottom panel) planes. Iso-contours represent the density of cluster members (orange), all field stars (gray) within the cluster's tidal radius, and 2000 field RRL stars (violet) within in a FOV of 20° around the cluster. A similar result is found when using proper motion in declination (not-shown). The analysis yields a final probability $(0.049 \pm 0.013)\%$ that the RRL is a chance interloper.

studied in this work. The distribution of field RRLs, although it includes thin and thick disc contributions (e.g. Mateu & Vivas 2018; Prudil et al. 2020), is dominated by halo RRLs, whose bulk kinematics differ significantly from the cluster's, which is kinematically associated to the thin disc.

We use a Gaussian Mixture to model the 3D distribution of proper motions and parallax of the background RRLs, we draw 500K random samples from the model and then compute the fraction whose proper motions and parallax coincide with the RRL star's to within 3 times its uncertainties and estimate the probability and its error as the mean and standard deviations from 100 bootstrap realisations. This yields a probability $p = (0.012 \pm 0.003)\%$. The final probability that such a star has been drawn at random in a sample of only four stars (the number of RRLs within the cluster's projected tidal radius) is given by the binomial probability of having one success in a sample of 4 draws when the probability of success is the p found above. This yields a final probability of $(0.049 \pm 0.013)\%$ that the RRL is a chance interloper. It is clear, then, the probability of the RRL in Trumpler 5 being a chance interloper is extremely low (1 in 2,000) and we take the association based on proper motions and parallax as a very robust one, even without the radial velocity information.

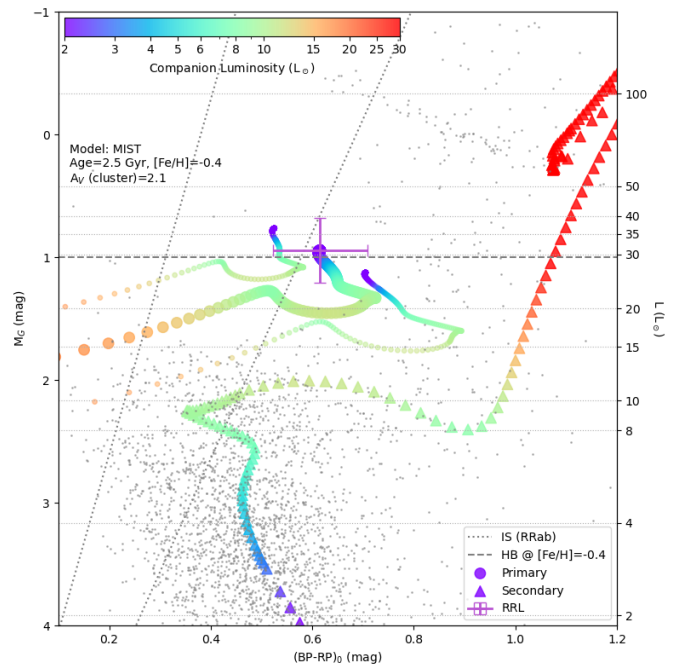


Fig. 4. CAMD for the cluster members (gray) and RRL (purple dot with error bars). Possible primary RRL stars are shown as coloured circles, and the corresponding secondary companions as triangles. The three tracks shown for primaries (from left to right) correspond to values of the assumed extinction, plus and minus its uncertainty. The colour scale represents the mass of the companion star. The IS limits for RRab from Cruz Reyes et al. (2024) and expected HB luminosity for the cluster's metallicity (as in Fig. 2) are shown by the dotted lines.

4. Discussion

4.1. Location in the CMD and constraints on binarity

We have established that the RRL star is a robust member of the Trumpler 5 cluster. The presence of an RRL star at such a young age (2–4 Gyr) is incompatible with single-star evolution models, and binary interactions have been suggested as a potential explanation (Iorio & Belokurov 2021; Bobrick et al. 2024; Sarbadhicary et al. 2021).

The lack of spectroscopic observations means that there is currently no direct evidence confirming (or ruling out) binarity. We analysed the *Gaia* RUWE parameter, which is consistent with a single star; however, this does not rule out low-mass and/or wide companions to which RUWE is not sensitive. The absence of visual companions only allows us to discard very wide binaries (an angular separation of $\sim 1''$ corresponds to ~ 1000 AU), which in any case would not be expected to have affected the evolution of the RRL. We now constrain the properties of a possible unresolved companion using photometry in two ways. First, we analyse the colour–absolute-magnitude diagram (CAMD) to estimate what type of companion could explain the position of the RRL star, slightly outside the empirical limits of the IS for RRab stars. Second, we explore the presence of excess emission in the spectral energy distribution (SED) that could arise from a companion or from circumstellar material.

Figure 4 shows the location of the Trumpler 5 RRL star in the CAMD using *Gaia* photometry. The absolute magnitude was computed from its intensity-averaged *G*-band magnitude from *Gaia* DR3 SOS (Clementini et al. 2023), its parallax distance including the -0.033 mas offset correction found by Garofalo et al. (2022) for RRL stars, and the interstellar extinction. The extinc-

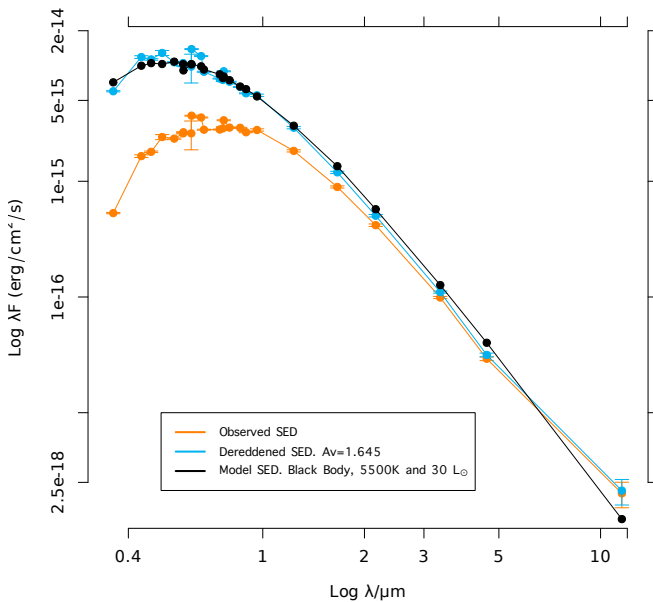


Fig. 5. Spectral energy distribution of the RRL best fitted to a black body with $T_{eff} = 5500K$ and $L = 30L_{\odot}$. The SED includes magnitudes in 24 pass-bands from 2MASS, Gaia DR3, HST/ACS, IPHAS, PS1, SDSS and WISE surveys. The SED was dereddened by $A_V = 1.645$ and the extinction law from Fitzpatrick (1999) and Indebetouw et al. (2005).

tion correction turns out to be the largest source of uncertainty in the calculation of M_G and color because the cluster suffers from strong differential reddening (Özdemir et al. 2025), which varies with distance and along different lines of sight. We therefore computed the extinction using the 3D extinction maps from Green et al. (2019) specifically for the line of sight and distance of the RRL, obtaining $A_V = 1.65$, which we converted to the extinction in the *Gaia* bands using Eq. A.1 in Appendix A.1 of Ramos et al. (2020).

The RRL star is located slightly outside the red edge of the instability strip for *RRab* from Cruz Reyes et al. (2024) and at the luminosity expected for the horizontal branch (HB) according to the Period–Luminosity–Metallicity (PLZ) relation from Garofalo et al. (2022) at the cluster’s metallicity. The colour offset suggests the possible presence of an unresolved companion, since the RRL star must lie inside the IS in order to develop its characteristic pulsation (e.g. Smith 1995). To explore constraints on a companion, we assume the observed source to be an unresolved binary in which the primary component is the RRL star inside the IS, and the secondary component is drawn from the normal cluster population so as to reproduce the observed position in the diagram. This exercise requires adopting an age for the cluster, which, as discussed by Özdemir et al. (2025), is uncertain when relying on photometry alone due to strong differential extinction and the resulting age–metallicity–extinction degeneracy. Using NIR spectroscopy, Özdemir et al. derived atmospheric parameters for several giant stars in the cluster, performed differential-reddening corrections, and obtained an age of 2.5 Gyr. They also presented a strong argument for this age: the clearly observed gap caused by the blueward hook in the isochrones near the main-sequence turn-off, a feature found only in populations this young. Therefore, in what follows we adopt their estimate of 2.5 Gyr for the cluster age.

Figure 4 shows the sequence of possible RRL primaries and their corresponding companions that reproduce the observed position of the unresolved binary, according to the MIST models (Dotter 2016; Choi et al. 2016). As the figure shows, main-sequence (MS) and subgiant branch (SGB) companions with masses $\lesssim 1.2 M_{\odot}$ have colours very similar or bluer to the RRL primary and either leave the colour of the RRL primary virtually unaffected or make it even redder, leaving the RRL primary outside the IS. This would disfavour any MS or SGB as probable companions, although, given the uncertainties, this cannot be completely ruled out.

The large uncertainty in extinction makes other configurations possible. At the highest limit of extinction (hottest and brightest position) the unresolved binary lies inside the IS. In this case, any MS companion would be consistent, only varying the implied luminosity of the RRL primary which would be in the range $25 \lesssim L/L_{\odot} \lesssim 35$. This scenario would be consistent with predictions from Bobrick et al. (2024) who used MESA stellar-population synthesis models including binary interactions to reproduce the production of young and metal-rich RRL stars. In their simulations, binary-made RRL stars are formed from evolved stripped-RGB stars and have surviving *main sequence* companions with masses between 0.65 and $1.9 M_{\odot}$ and luminosities $15 \lesssim L/L_{\odot} \lesssim 35$. Initial masses for binary-made RRL stars are found to be in the range 0.95 – $2 M_{\odot}$ with mild mass ratios between 1.0 and 1.55. Because the primary is the star that becomes an RRL after ascending the RGB, its initial mass correlates with the age of the population. Since the mass ratios do not span a very large range, Bobrick et al. (2024) point out that the secondary mass also roughly correlates with age, with systems younger than 3 Gyr having companion masses larger than $1 M_{\odot}$. This would be consistent with our Trumpler 5 RRL for extinctions at the upper end range allowed by uncertainties and with luminosities at the higher end of the range predicted by Bobrick et al. (2024).

The last possible case arises if the unresolved binary is placed at the lowest limit of extinction, (coolest and faintest position). In this scenario, the only possible companion is an RGB star with more than $\sim 30 L_{\odot}$. Although this scenario has been proposed to explain Yellow Straggler stars (YSS, see next subsection) a companion with such a high luminosity and low temperature ($\sim 3500 K$) would produce an excess in the SED of the observed RRL star at wavelength $\lambda > 1 \mu m$, a feature which is not observed.

Figure 5 shows the dereddened SED for the RRL star built using the VOSA tool (Bayo et al. 2008) and literature photometry over the wavelength range $0.36 \lesssim \lambda/\mu m \lesssim 11$. The SED fits well to a single blackbody of $T_{eff} = 5700$ K with a luminosity $L = 33 L_{\odot}$ over the complete wavelength range, and the same result is obtained when fitting only the optical wavelengths ($\lambda \lesssim 1.2 \mu m$). This result rules out a luminous RGB companion and also suggests the absence of IR excesses up to $\lambda \lesssim 11 \mu m$ from circumstellar material. The best fit to a two-blackbody model results in two indistinguishable components with $T_{eff} = 5700$ K and $L = 16 L_{\odot}$ each. Although the result supports the T_{eff} previously found it is not sensitive to companions with luminosities well below that of the RRL star, as the resulting changes are comparable to the photometric uncertainties.

In summary, the observed RRL has the luminosity of a normal RRL but a redder colour which is consistent with the presence of a companion that makes the primary RRL fainter as predicted by current binary interactions models. Although we cannot place definitive constraints on the presence of such a companion from the CAMD and the SED, if exists, it is probably a

SGB or RGB depending on the extinction. We note that available interferometric observations with angular resolutions and sensitivity to resolve even faint companions at angular distances of tenths of mas could probe for companion at distances from 30 to 300 AU.

4.2. A binary-friendly cluster

The Trumpler 5 RRL was also identified by Rain et al. (2021) as a member of this cluster using the OC members from Cantat-Gaudin et al. (2018, 2020), and classified it as a *yellow straggler star* (YSSs), one of the *two* found in the cluster. In their work, YSSs are defined as stars redder than the main sequence turn-off, bluer than the red giant branch and more luminous than the subgiant branch, conditions indeed met by our star. In addition to the possibility of them being unresolved binaries whose combined fluxes place them in the YSS locus (Rain et al. 2021; Mermilliod et al. 2007), YSSs are of special interest since it has also been proposed they may have been formed by binary mergers, collisions and/or mass transfer from a red giant companion (Landsman & Stecher 1997; Landsman & Simon 1998; Leiner et al. 2016).

Rain et al. (2021) also found 103 *blue straggler stars* (BSSs) in Trumpler 5, making it the OC with the largest absolute population of BSSs and the 8th in terms of its relative fraction, calculated as the fraction of BSSs relative to main sequence stars up to 1 mag below the turn-off. The correlation between the fraction of BSSs and the binary fraction of a population observed in open and globular clusters as well as in dwarf galaxies (e.g. Ferraro et al. 2025; Momany 2015) implies Trumpler 5 hosts a relatively large population of binaries in comparison to other OCs.

If binary evolution with mass transfer is indeed a viable evolutionary path for RRLs to be produced at intermediate ages, the relatively large mass of Trumpler 5 ($> 24,000 M_{\odot}$) combined with a comparatively large binary fraction could arguably ‘conspire’ favourably for the cluster to have produced a binary-evolution RRL despite how inefficient this mechanism may be.

It should also be noticed that Trumpler 5 is an atypical OC, being older and more metal-poor than typical OCs (Özdemir et al. 2025), and with a mass larger than the canonical mass of OCs (Portegies Zwart et al. 2010). Trumpler 5 is a dynamically evolved cluster as shown by an analysis of the profile of its BSSs (Rain et al. 2020), with a mass resembling that of a low-mass Young Massive Cluster (YMC), leading to think this could be a transition cluster between OC and YMC, considering OCs as the low-mass end of YMCs (Bastian 2016).

5. Conclusions

In this work we have provided *the first conclusive association of an RRL to an intermediate-age star cluster: the 2–4 Gyr-old Trumpler 5*.

We have shown the star to be a bona fide RRL, identified independently and consistently by five RRL surveys: Gaia DR3 SOS, ASAS-SN, PS1, ZTF and OGLE-IV. Its full information, as well as the cluster’s, is provided in Table 1. The star was robustly identified as a member of the Trumpler 5 cluster by Hunt & Reffert (2024); Cantat-Gaudin et al. (2018) and Cantat-Gaudin et al. (2020), it is located within the cluster’s tidal radius, and its proper motions and parallax are in remarkable agreement with the cluster’s members. Its observed apparent G-band magnitude is consistent with the expectation for the HB at the cluster’s metallicity and at the star’s distance and extinction according

to the Green et al. (2019) dust map. Based on the parallax and proper motion distribution of field RRL stars and the total number of field RRLs observed within the cluster’s tidal radius (3), we have shown the RRL to have a probability of $0.049 \pm 0.013\%$ of randomly sharing the cluster’s parallax and proper motion to within 3 times the star’s uncertainties, implying a very low chance of the RRL being a chance interloper. Given the size of the cluster sample ($> 3K$ OCs) searched (Hunt & Reffert 2024), having observed one RRL in the 1–8 Gyr age range agrees, to within Poisson noise, with the ~ 2 expected from the PTF results obtained by Cuevas-Otahola et al. (2025) from LMC clusters.

Finally, although not firmly conclusive due to the large extinction uncertainties, we explored possible constraints on a binary companion based on the CAMD and the star’s SED. Its location just outside the red edge of the IS suggests the need for a binary companion such that the primary star responsible for the RRL pulsation would lie inside the IS. In this case and with an extinction lower than or equal to the assumed $A_V = 1.65$ from the Green et al. (2019) dust map, the most likely scenarios would require for the secondary companion to be either a subgiant or red giant star at the base of the RGB ($8 \lesssim L/L_{\odot} \lesssim 12$), which would produce under-luminous RRLs compared to the expectation for the cluster’s metallicity. If the extinction were larger, the observed star would lie inside the IS and either be consistent with a single star or with MS companions of any mass, making the RRL slightly over-luminous for its metallicity, and subgiant and red giant companions up to $L \lesssim 10L_{\odot}$.

The association of an RRL star to Trumpler 5, a decidedly intermediate-age simple stellar population, is the most direct evidence so far of the existence of these ‘young’ RRLs and adds firm support to the evidence that has been systematically accumulating toward the existence of RRL stars at these unusual ages, both in the MW and LMC (Iorio & Belokurov 2021; Sarbadhicary et al. 2021; Zhang et al. 2025; Cabrera-Gadea et al. 2025).

Acknowledgements. CM is delighted to thank Pau Ramos and Danny Horta for useful discussions and early readings of the manuscript. JJD and BCO acknowledge support from the RDT funding from Universidad de la Repùblica, Uruguay. This work has made use of data from the European Space Agency (ESA) mission *Gaia* (<https://www.cosmos.esa.int/gaia>), processed by the *Gaia* Data Processing and Analysis Consortium (DPAC, <https://www.cosmos.esa.int/web/gaia/dpac/consortium>). Funding for the DPAC has been provided by national institutions, in particular the institutions participating in the *Gaia* Multilateral Agreement.

References

- Anderson, R. I. & Hunt, E. L. 2025, A&A, 700, L13
- Bastian, N. 2016, in EAS Publications Series, Vol. 80-81, EAS Publications Series, ed. E. Moraux, Y. Lebreton, & C. Charbonnel, 5–37
- Bayo, A., Rodríguez, C., Barrado Y Navascués, D., et al. 2008, A&A, 492, 277
- Bobrick, A., Iorio, G., Belokurov, V., et al. 2024, MNRAS, 527, 12196
- Cabrera-Gadea, M., Mateu, C., & Ramos, P. 2025, A&A, 701, A136
- Cantat-Gaudin, T., Anders, F., Castro-Ginard, A., et al. 2020, A&A, 640, A1
- Cantat-Gaudin, T., Jordi, C., Vallenari, A., et al. 2018, A&A, 618, A93
- Catelan, M. & Smith, H. A. 2015, Pulsating Stars, 1st edn. (Weinheim, Bergstr: Wiley-VCH)
- Chen, X., Wang, S., Deng, L., et al. 2020, ApJS, 249, 18
- Choi, J., Dotter, A., Conroy, C., et al. 2016, ApJ, 823, 102
- Clementini, G., Ripepi, V., Garofalo, A., et al. 2023, A&A, 674, A18
- Cruz Reyes, M., Anderson, R. I., Johansson, L., Netzel, H., & Medaric, Z. 2024, A&A, 684, A173
- Cuevas-Otahola, B., Mateu, C., Cabrera-Ziri, I., et al. 2025, MNRAS, 541, 1434
- Dias, W. S., Monteiro, H., Moitinho, A., et al. 2021, MNRAS, 504, 356
- Donati, P., Cocozza, G., Bragaglia, A., et al. 2015, MNRAS, 446, 1411
- D’Orazi, V., Storm, N., Casey, A. R., et al. 2024, MNRAS, 531, 137
- Dotter, A. 2016, ApJS, 222, 8
- Ferraro, F. R., Lanzoni, B., Vesperini, E., et al. 2025, arXiv e-prints, arXiv:2506.07692

Fitzpatrick, E. L. 1999, PASP, 111, 63

Gaia Collaboration, Brown, A. G. A., Vallenari, A., et al. 2018, A&A, 616, A1

Gaia Collaboration, Vallenari, A., Brown, A. G. A., et al. 2023, A&A, 674, A1

Garofalo, A., Delgado, H. E., Sarro, L. M., et al. 2022, MNRAS, 513, 788

Green, G. M., Schlafly, E., Zucker, C., Speagle, J. S., & Finkbeiner, D. 2019, ApJ, 887, 93

He, S.-X., Huang, Y., Li, X.-Y., et al. 2025, ApJS, 278, 2

Hunt, E. L. & Reffert, S. 2023, A&A, 673, A114

Hunt, E. L. & Reffert, S. 2024, A&A, 686, A42

Indebetouw, R., Mathis, J. S., Babler, B. L., et al. 2005, ApJ, 619, 931

Iorio, G. & Belokurov, V. 2021, MNRAS, 502, 5686

Jayasinghe, T., Stanek, K. Z., Kochanek, C. S., et al. 2019a, MNRAS, 486, 1907

Jayasinghe, T., Stanek, K. Z., Kochanek, C. S., et al. 2019b, MNRAS, 485, 961

Karczewski, P., Wiktorowicz, G., Ilkiewicz, K., et al. 2017, MNRAS, 466, 2842

Kinman, T. D. & Brown, W. R. 2010, AJ, 139, 2014

Landsman, W. & Simon, T. 1998, in American Astronomical Society Meeting Abstracts, Vol. 193, American Astronomical Society Meeting Abstracts, 37.03

Landsman, W. & Stecher, T. P. 1997, in American Institute of Physics Conference Series, Vol. 408, The ultraviolet universe at low and High redshift, ed. W. H. Waller, 390–394

Leiner, E., Mathieu, R. D., Stello, D., Vanderburg, A., & Sandquist, E. 2016, ApJ, 832, L13

Li, X.-Y., Huang, Y., Liu, G.-C., Beers, T. C., & Zhang, H.-W. 2023, ApJ, 944, 88

Lindegren, L. 2018, gAIA-C3-TN-LU-LL-124

Mateu, C. & Vivas, A. K. 2018, MNRAS, 479, 211

Medina, G. E., Muñoz, R. R., Carlin, J. L., et al. 2024, MNRAS, 531, 4762

Mermilliod, J. C., Andersen, J., Latham, D. W., & Mayor, M. 2007, A&A, 473, 829

Momany, Y. 2015, in Astrophysics and Space Science Library, Vol. 413, Astrophysics and Space Science Library, ed. H. M. J. Boffin, G. Carraro, & G. Beccari, 129

Muraveva, T., Giannetti, A., Clementini, G., Garofalo, A., & Monti, L. 2025, MNRAS, 536, 2749

Ngeow, C.-C. & Bhardwaj, A. 2025, AJ, 169, 156

Özdemir, S., Afsar, M., Sneden, C., et al. 2025, A&A, 699, A208

Portegies Zwart, S. F., McMillan, S. L. W., & Gieles, M. 2010, ARA&A, 48, 431

Prudil, Z., Debattista, V. P., Bernaldo de Silva, L., et al. 2025, A&A, 699, A349

Prudil, Z., Dékány, I., Grebel, E. K., & Kunder, A. 2020, MNRAS, 492, 3408

Rain, M. J., Ahumada, J. A., & Carraro, G. 2021, A&A, 650, A67

Rain, M. J., Carraro, G., Ahumada, J. A., et al. 2020, The Astronomical Journal, 161, 37

Ramos, P., Mateu, C., Antoja, T., et al. 2020, A&A, 638, A104

Sarbadhicary, S. K., Heiger, M., Badenes, C., et al. 2021, The Astrophysical Journal, 912, 140

Sesar, B., Hermitzschek, N., Dierickx, M. I. P., Fardal, M. A., & Rix, H.-W. 2017a, ApJ, 844, L4

Sesar, B., Hermitzschek, N., Mitrović, S., et al. 2017b, AJ, 153, 204

Smith, H. A. 1995, RR Lyrae Stars, Cambridge Astrophysics Series

Soszyński, I., Udalski, A., Szymański, M. K., et al. 2016, Acta Astron., 66, 131

van Groeningen, M. G. J., Castro-Ginard, A., Brown, A. G. A., Casamiquela, L., & Jordi, C. 2023, A&A, 675, A68

Zhang, H., Iorio, G., Belokurov, V., et al. 2025, arXiv e-prints, arXiv:2504.06720

Appendix A: Discarded stars

The search for RRL members in OCs yielded an initial sample of 15 stars. Here we discuss the 14 stars which we discarded as misclassified RRLs, mainly based on the appearance of their phase-folded light curves and/or position in the CAMD. Figure A.1 shows the phase-folded light curves for all the time series publicly available from *Gaia*, ASAS-SN, PS1 and OGLE-IV for these stars. In this plot, stars C13 and C14 were identified as RRLs by ZTF alone. Since the ZTF time series are not available, we show the *Gaia* DR3 for C13. We were unable to find any time series information for star C14, hence it is not shown in Fig. A.1. Figure A.2 shows the proper motion plane, parallax histogram, CAMD and Period-Amplitude diagram for the star of interest (purple star) and cluster members from Hunt & Reffert (2023), similarly to Fig. 2. Table A.1 summarises the available light curve information for the discarded stars.

Since the RRLs we are interested in could belong to unresolved binaries we should not, a priori, rule out stars that lie outside the IS. We can, however, discard any stars below the expected HB luminosity since an unresolved binary can only be more luminous than the RRL, assuming it has a ‘normal’ luminosity. The position in the CAMD of Fig. A.2 for several stars (e.g. C5, C6, etc.) places them well below the HB and, in many cases, directly on the MS. These cases are denoted as below-HB/MS in the comments of Table A.1 as reasons for the stars to be discarded from our sample. In what follows we describe the criteria used to discard each star, also summarised in Table A.1.

Stars C1, C2, C3, C4, show the characteristic light curves of contact or semi-detached eclipsing binaries (W UMa/EW and β Lyr/E β), consistent with their position on or near the MS as seen in the CAMD of Figure A.2. Star C5 has a very noisy light curve and is placed well below the MS. Stars C6, C8, C9, C10 and C11 have reasonably well behaved light curves, but too short amplitudes much more consistent with being either δ Scuti stars or eclipsing binary (EB), the latter being more consistent with their position in the MS but outside the IS, in the CAMD. Star C7 is bluer than the IS and more luminous than the HB, which would make it a good candidate, except for its extremely low amplitude, particularly for its period, and the significant gap in its light curve. This star might be worth revisiting, but for now it is discarded as a possible EB. Stars C12 and C13 show almost constant light curves with a few deviated points, usually characteristic of detached eclipsing binaries (Algol/EA). This is indicated with the corresponding variability classification in the comments of Table A.1. Finally, star C14 has a very short amplitude and is located right at the MS, well below the HB. Although it is the only star without time series data available, its very short amplitudes and location in the CAMD make it likely to be an EB.

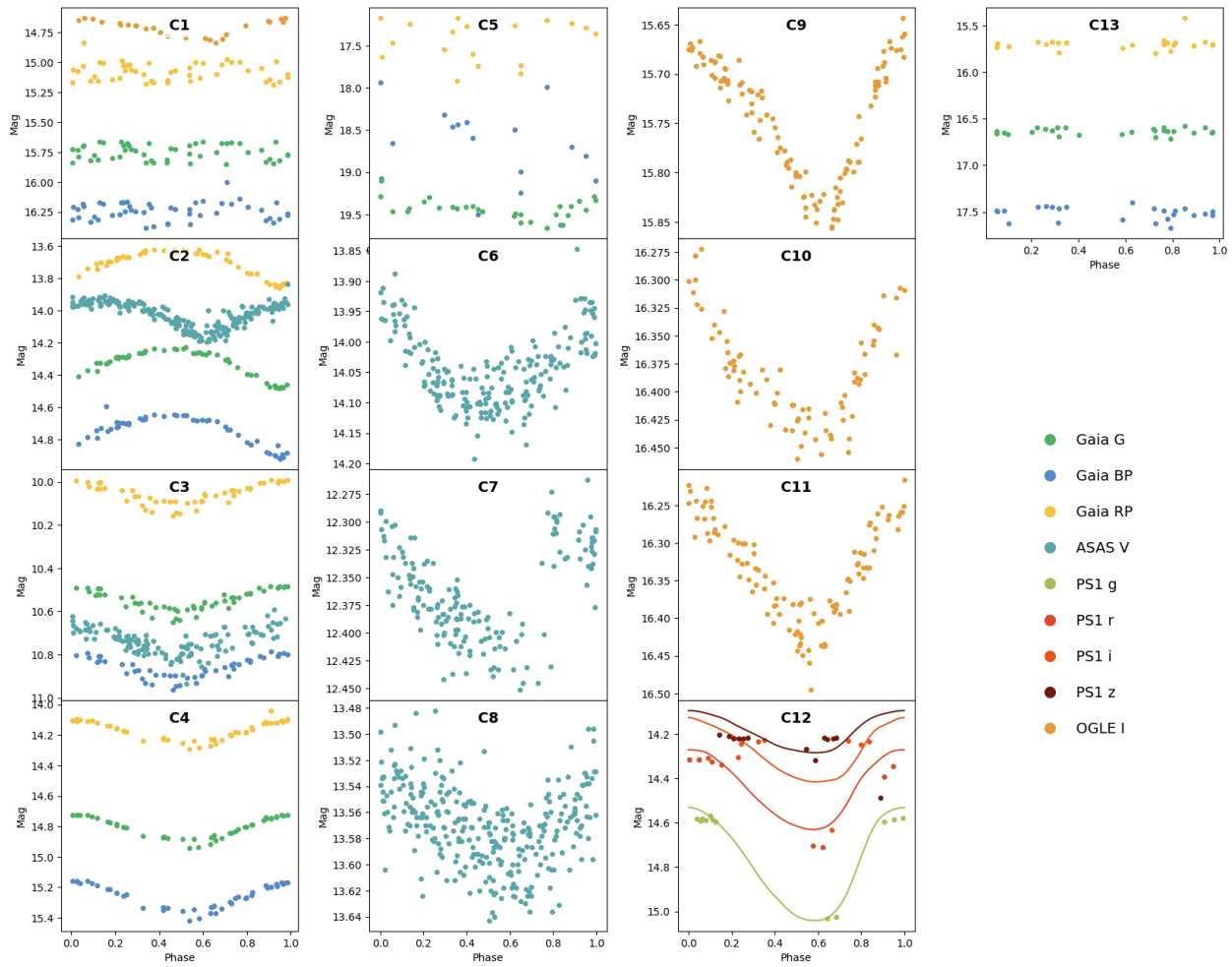


Fig. A.1. Phase folded light curves for each of the 13 out of 14 stars discarded from the sample, with available time series data. Star 3330383474578837248 is not shown as it was identified by ZTF alone and its time series data is not publicly available, not does it have time series information in *Gaia* DR3.

ID	Gaia Source ID	Periods (d) (G,A,O)	Amplitudes (mag) (BP,RP,G,V,I)	Comments
C1	5594538779611595136	(--, 0.7541)	(--,--, 0.18)	EW, MS
C2	5533487296963447552	(-, 0.2792,--)	(--,--, 0.23,--)	EW, MS
C3	2012045019718073728	(-, 0.4310,--)	(--,--, 0.18,--)	EW, MS
C4	2004077065120273664	(0.8335,--,--)	(0.21, 0.16, 0.18,--,--)	EW, MS
C5	5534158205211222144	(0.3622,--,--)	(0.80, 0.27, 0.27,--,--)	noisy, below-HB
C6	5585551027962400384	(-, 0.4400,--)	(--,--, 0.17,--)	EB, MS
C7	511219584907760896	(-, 0.4992,--)	(--,--, 0.13,--)	off-MS, short Amp
C8	5294043694838471552	(-, 0.7017,--)	(--,--, 0.09,--)	EB, MS
C9	5616530661434711680	(--, 0.7728)	(--,--,--, 0.17)	EB, MS
C10	5957810991851847296	(--, 0.3583)	(--,--,--, 0.13)	EB, MS
C11	4085159414905583104	(--, 0.4053)	(--,--,--, 0.17)	EB, MS
(PS1) (g,r,i,z)				
C12	3355237350809737344	(0.2723)	(0.51, 0.36, 0.29, 0.19)	constant/EA?
(ZTF) (g,r)				
C13	182831054077294336	(0.8605)	(0.10,0.10)	constant/EA?
C14	3330383474578837248	(0.3134)	(0.19,0.12)	MS, below-HB

Table A.1. Stars discarded as misclassified RRLs.

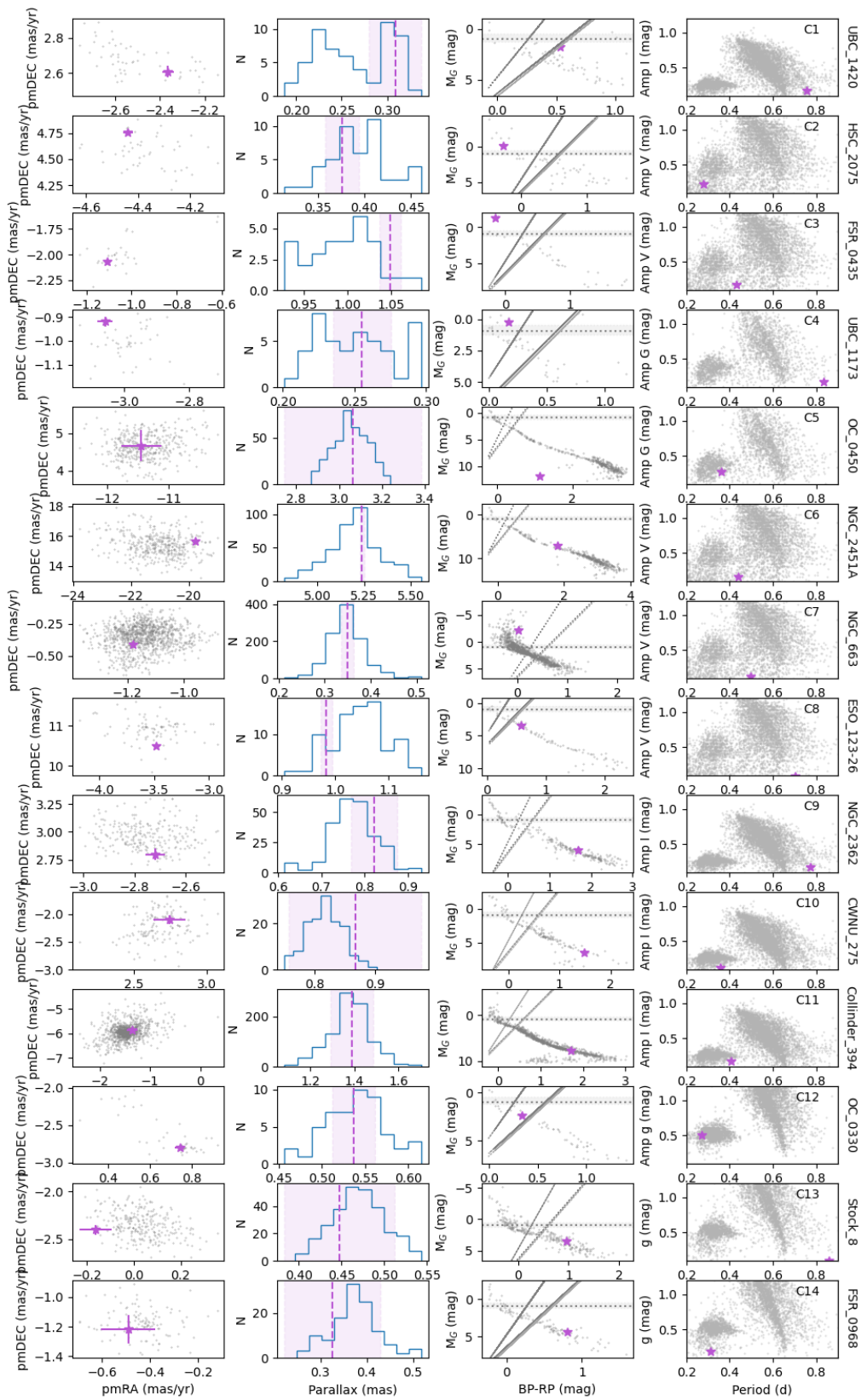


Fig. A.2. Discarded RRL stars (purple star) and cluster members (light gray) are shown, from left to right, in the plane of proper motions (pmDEC versus pmRA), parallax, *Gaia* CAMD and Period-Amplitude diagram. In the CAMD, the solid lines correspond to IS limits from Cruz Reyes et al. (2024) with He abundances from $Y = 0.22$ to $Y = 0.395$; the dotted line shows the *expected* location of the HB at each cluster's metallicity from Garofalo et al. (2022), and its distance and extinction according to Hunt & Reffert (2024); the shading represents the uncertainty in the HB luminosity corresponding to $\Delta[\text{Fe}/\text{H}] = 0.5$ dex. The star's ID from Table A.1 and the cluster's name are shown in the fourth panel top right corner and Y axis, respectively.